Understanding propulsive shoulder forces and scapular kinematics during manual wheelchair use

Dr Tom Paulson[1], Dr Dylan Morrissey[2,3], Dr Barry Mason[1], Dr Riemer Vegter[1,4], Dr Bertrand Bru[5], Prof. Lucas van der Woude[1,4] & Prof. Victoria Goosey-Tolfrey[1]

[1]The Peter Harrison Centre for Disability Sport (PHC), School of Sport, Exercise and Health Sciences, Loughborough University, Loughborough, UK

[2]Sport and Exercise Medicine, Queen Mary University of London, UK

[3]Physiotherapy Department, Bart's Health NHS Trust, London, UK

[4]University of Groningen, University Medical Centre Groningen, Groningen, The Netherlands

[5]Charnwood Dynamics Ltd, Codamotion, Rothley, Leicestershire, UK

Executive Summary

Introduction Shoulder pain and inefficient propulsion are common and disabling problems for wheelchair users, yet little is known about how the interaction between wheelchair configuration and users affects shoulder girdle biomechanics. This can impact significantly on performance during activities of daily living (ADL) and sport. This PMG research grant, matched with PHC funds, enabled us to assemble an inter-disciplinary team with expertise focussed on accurately measuring the shoulder forces (kinetics) and movements (kinematics) during manual wheelchair propulsion. The aim was to establish a feasible and reliable method that could be employed to better understand how manipulating wheelchair configurations can minimise future shoulder girdle pain and pathology.

Method We recruited 10 active males, manual wheelchair-reliant for both ADL and sport (n=5 with shoulder pain, of which n= 3 unilateral). Each participant performed six 4-min submaximal bouts (3, 4 and 6 $km.h^{-1}$ (T1), repeated following a 20 min rest (T2)) in their personal ADL wheelchair mounted on a wheelchair ergometer. An instrumented measurement wheel examined propulsion kinetics and technique parameters while three-dimensional kinematic analysis was used to assess bilateral scapulothoracic rotations (internal/external and upward/downward, anterior/posterior tilt) over propulsive cycles. Differences across speeds for the aforementioned parameters were assessed using one-way repeated measures ANOVA with Tukey post-hoc tests. Bilateral asymmetries in scapular kinematics were investigated with respect to self-reported shoulder pain and the intra-investigator reliability (T1 vs T2) of the scapular kinematic technique was computed using typical error (TE) and intraclass correlation coefficient (ICC) statistics.

Results Push frequency, peak force, contact angle, cycle time and power output were all significantly different between each propulsion speed ($p<0.05$; Effect size = 0.38 to 0.98). Common to all speeds was an internally rotated and anteriorly tilted scapula. Peak internal rotation of the scapula occurred during the recovery phase of the propulsion cycle and the scapula moved towards a neutral or posteriorly tilted position at ~50% propulsion cycle. Mean (~3º) and peak (~4º) scapular internal rotations were significantly greater at 6 $km.h^{-1}$ than either of the other speeds. Intra-investigator reliability for the scapular kinematics was: TE = 1.6 to 3.1º; ICC = 0.87-0.97. Absolute bilateral asymmetries ranged from 0.5º-16.7º, 0.4º-11.6º and 0.9º-10.7º for internal, upward rotation and anterior/posterior tilt respectively. Large intra-individual variability was present for bilateral asymmetry with no association between scapular kinematics and self-reported pain symptoms.

Future work This work has established methods and generated an initial database to enable future work understanding how wheelchair configurations can be manipulated to prevent shoulder girdle pain and improve propulsive efficiency. Furthermore we have developed a robust measurement protocol which can be refined to generate real time information assessing the effectiveness of future wheelchair configuration interventions.

Background

For the ~1.2 million wheelchair users in the UK, wheeled mobility is an essential requirement for leading an active role in society and preserving quality of life ('Right chair, right now' NHS improving quality 2014). However, with the limited muscle mass and low stability but high mobility of the shoulder girdle (Veeger & van der Helm 2007), manual wheelchair use (MWU) is associated with substantial risk of chronic upper-extremity (UE) pain and injury (Nichols et al. 1979; Curtis et al. 1999). The appropriate provision and configuration of a manual wheelchair is imperative to reduce the risk of injury and shoulder pathology in MWU and maintain both physical and mental well-being ('Right chair, right now' NHS improving quality 2014). A greater evidence base supported by well-designed, scientific data collection could support services responsible for wheelchair prescription to prioritise pain reduction and minimise secondary conditions associated with regular wheelchair use.

Introduction

UE pain is reportedly present in 40-70% of MWU with a spinal cord injury (SCI) (Curtis et al. 1999), with 30-40% of individuals experiencing pain during and within the 1st year after rehabilitation (Eriks Hoogland et al. 2016; van Drongelen et al. 2006). Brose et al. (2008) observed an extremely high prevalence of supraspinatus tendinopathy (100%) and impingement (91.8%) in 49 active MWU with paraplegia, with 67% symptomatic for pain. Similarly, Medina et al. (2015) observed a similarly high prevalence of rotator cuff tendinopathy (>80%), bursitis (>55%) and acromioclavicular joint degeneration (>60%) in both active and sedentary males with tetraplegia. Mechanical impingement of the soft-tissue residing within the subacromial space of the glenohumoral (GH) joint (e.g. rotator cuff muscles, bicep tendon) is therefore considered a primary cause of shoulder pain and overuse pathology in MWU (Brose et al. 2008; Medina et al. 2015; van Drongelen et al. 2006).

Central to impingement risk is the orientation of the scapula, with increased internal rotation, decreased upward rotation (increased downward rotation) and increased anterior tilt associated with reduced subacromial space (Kilber et al. 2013). Large peak GH reaction forces (300-1400N) are observed during manual wheelchair propulsion (Arnet et al. 2012), resulting in the repetitive and forceful elevation of the humeral head into the subacromial space (Veeger et al. 2002). High muscle forces are also observed in the rotator cuff muscles, especially m. supraspinatus (Veeger et al. 2002). These forces acting on the shoulder girdle structure coupled with 'high risk' scapular kinematics observed during manual propulsion (Morrow et al. 2011; Raina et al. 2012; Zhao et al. 2014) likely contribute significantly to pain pathology in MWU. In addition, impaired UE muscle innervation of individuals with tetraplegia may lead to reduced scapula control and a greater rate of change in scapular motion during dynamic activity (Raina et al. 2012). This increased impingement risk may reflect the higher prevalence of shoulder pain in individuals with higher SCI (Curtis et al. 1999; Medina et al. 2015; van Drongelen et al. 2006).

Due to its broad, flat shape, substantial soft-tissue covering and subsequent skin motion artefact during dynamic activity, the scapula is difficult to track using motion capture technology (Karduna et al. 2001; van Andel et al. 2009). A clinically feasible method of quantifying scapular motion requires unconstrained measurements to maximise ecological validity and minimise compensatory movements, therefore excluding the 'gold-standard' and highly-invasive bone-pin measurement during wheelchair propulsion. Previously, Karduna et al. (2001) confirmed the validity of non-invasive, skin-based scapular locator and acromion-mounted sensors for quantifying 3-D scapular kinematics during arm elevation. The reliability of the acromion marker cluster (AMC) technique method was confirmed by van Andel et al. (2009) during the same movement below humerus elevations of 100˚. Subsequently, the AMC technique has been frequently employed during manual propulsion and tasks of daily living (Raina et al. 2012; Vegter et al. 2013; Zhao et al 2014). However, no standard marker cluster is currently available and the reliability of an AMC method should be confirmed for each movement pattern investigated. This is especially important where contracting muscle and skin vibrations surrounding the AMC may influence the measurements during dynamic propulsion or impaired UE function secondary to a SCI may alter scapular control.

A high proportion of self-reported shoulder pain is unilateral in nature (Curtis et al. 1999). As a bilateral task, manual propulsion challenges UE motor control when repeatedly coupling the hand-rim and maintaining a linear direction of travel (Vegter et al. 2013). Despite this, the reporting of bilateral data in wheelchair propulsion literature is limited, often due to increased cost of equipment for data collection or the 'assumption' of symmetry in UE kinetics and kinematics. Even with bilateral data collection, studies often do not report results for both sides, they are either averaged or just reported for a single limb (Boninger et al. 2002). However, Boninger et al. (2002) previously observed around 40% of a subset of MWU with paraplegia displayed bilateral asymmetries in hand recovery pattern during a propulsion cycle. Hurd et al. (2008) reported significant asymmetries in force and timing parameters in 12 MWU's free from pain, with increased magnitudes during propulsion up ramps and on uneven surfaces. In contrast, Soltau et al. (2015) found no difference in propulsion kinetics in 80 MWU with paraplegia, with only small differences in hand contact angle. Side to side differences (~5˚) in joint range of motion were observed but these were smaller than differences between individuals and therefore not considered clinically meaningful (Soltau et al. 2015). However, even small differences in moments or forces may result in cumulative differences during repetitive MWU and risk factors for unilateral pain in manual users have not yet been identified. Defining a range of scapular kinematic asymmetry may also be a useful tool when supporting the configuration and postural assessment of MWU and understanding shoulder girdle pathology.

The overall aim of this project was to establish methods for the multi-system measurement of shoulder motion during three submaximal speeds of wheelchair propulsion. Specifically the following report will:1) Examine forces acting on the shoulder girdle, movement patterns of the scapula and technique-related parameters during submaximal manual propulsion in a daily use wheelchair; 2) Examine asymmetries in scapular motion within individuals and in relation to the presence of pain during tasks of daily living; and 3) Assess the intra-observer reliability of the technique for performing kinematic analysis of the scapula and how this may influence the quantification of forces acting on the shoulder.

Methods

Participants

Ten active males with a mean age of 34.0 ± 4.8 yrs and body mass of 69.5 ± 5.1 kg participated in the research after providing written informed consent. Eight participants presented a motor complete (ASIA A and B) cervical spinal cord injury (C5-C8), one presented with cerebral palsy and 1 presented sensorimotor polyneuropathy. Further participant details are provided in **Table 1**. The feasibility study was approved by Loughborough Universities ethics sub-committee (REF R15-P161 05/01/2015). Criteria for inclusion were: reliance on a manually propelled wheelchair for both activities of daily living and recreation, at least 3 years' experience of manual wheelchair propulsion and successful completion of the Health Screen Questionnaire approved by the Local ethical advisory committee. Criteria for exclusion were: the presence of severe medical conditions including hypertension, cardiovascular disease and skin irritations/pressure sores.

Table 1 Participant characteristics

Participant	Age (yrs)	Body Mass (kg)	Chair mass + wheels (kg)	Time as MWU (yrs)	WUSPI	PSQ Shoulder (Left/Right)	PSQ Elbow (Left/Right)	PSQ Neck
1	34	73.6	11.8	3	39	15/15	2/2	6
2	28	66.0	15.3	9	27	6/9	0/0	4
3	34	72.2	13.6	6	4	0/0	15/15	0
4	36	72.5	12.6	13	1	0/0	0/9	4
5	39	80.0	12.5	22	1	0/0	0/4	0
6	31	64.1	12.5	31	0	0/0	0/0	0
7	31	67.1	11.9	9	4	0/0	0/0	0
8	28	69.2	11.8	4	4	2/0	0/0	0
9	36	64.9	12.5	20	4	2/0	0/0	1
10	43	65.0	10.1	26	22	9/0	0/0	9
Mean (SD)	**34 (5)**	**69.5 (5.1)**	**12.5 (1.3)**	**14 (10)**	**10 (13)**	**-**	**-**	**-**

n.b. n=10 participants were right hand dominant. MWU = manual wheelchair user; WUSPI = wheelchair users shoulder pain index; PSQ = upper-extremity pain symptom questionnaire; SD = standard deviation.

Experimental protocol

On arrival, all participants completed the Wheelchair Users Shoulder Pain Index (WUSPI) (Curtis et al. 1995) and an upper-extremity pain symptom questionnaire (PSQ) (van Drongelen et al. 2006). The WUSPI required participants to rate the severity of shoulder pain experienced during 15 tasks of daily living over the preceding 7 days using a 10 cm visual analogy scale (0= no pain; 10 = worst pain ever experienced). A score of 150 indicates the highest pain score possible, with zero indicating no pain. The PSQ required participants to rate the severity (1 = 'very mild' to 5 = 'very severe') and frequency (1 = 'once a week or less' to 3 = > 3 times per week') of bilateral musculoskeletal pain for fingers/wrist, elbow, shoulders and neck in the last 3 months. An overall total for each limb was calculated by multiplying the severity and frequency of pain.

Subsequently, participants transferred to an upright chair and sat in a comfortable position while 24 active markers were attached to both limbs via double sided medical-grade adhesive tape. The tracked bony landmarks (real and virtual) were chosen so the segment orientations and joint angles could be calculated as recommended by the International Society of Biomechanics (ISB) (Wu et al. 2005). Single markers were attached to the thorax at C7, T8, Incisura Jugularis and the process Xiphoideus (**Appendix 1**). Medial/lateral humeral epicondyles (ME and LE), ulna styloids and radial styloids were recorded during a static acquisition. Their positions were calculated based on the position their related technical cluster during dynamic trials (Cappozzo et al., 1995). Technical markers (consisting of 4 single markers in different rigid body configurations) were placed on the forearm, upper arm and on the flat superior surface of the posteromedial aspect of the acromion (**Appendix 1**). The position of the Coracoid Process (PC), Acromioclavicular joint (AC), Trigonum Spinae Scapulae (TS), Angulus Acromialis (AA) and Angulus Inferior (AI) of the scapula were recorded during a static trial. Their positions were reconstructed during the dynamic trials using the position acromion tetrads (Cappozzo et al., 1995) and were used to calculate the theoretical position of the glenohumeral joint centres using the Meskers's regression equation (Meskers et al., 1998). Data were collected at 100Hz using four Coda CX1 units and Odin software (Charnwood Dynamics Ltd., Codamotion, Rothley, Leicestershire, UK).

All testing was performed in the participant's daily wheelchair mounted on a dual-roller ergometer (VP Handisoft-25, Medical Development HEF Groupe, Andreziuex Boutheon, France) (**Appendix 1)**. Each participant completed 3 continuous, submaximal exercise trials at speeds consistent with activities of daily living (3, 4 and 6 $km \cdot h^{-1}$) with 2 min rest between stages (T1). On-line respiratory gas analysis was performed throughout each 3-min stage via a breath-by-breath system (Cortex metalyser 3B, Cortex, Leipzig, Germany) and values of oxygen uptake (VO2) and the respiration exchange ratio (RER) were averaged over the final 60 sec of each trial. Before each test, gases were calibrated according to the manufacturers recommendations using a 2-point calibration (O_2 = 17.0%, CO_2 = 5.0% against room air) and volumes with a 3-L syringe at flow rates of 0.5–3.0 $L{\cdot}s^{-1}$. Mechanical efficiency was derived from the ratio between the external power output (W) and the energetic equivalent for oxygen (W) (Whipp and Wassrman 1969). Participant's subjective rating of perceived exertion using Borg 6-20 scale was also recorded.

Following a 20 min rest period, the 3 submaximal trials were repeated (T2) in the same order as performed previously. During the rest period the active joint markers were removed by a neutral investigator and re-applied by the same investigator as T1. Subsequently, the positions of the anatomical landmarks relative to the technical markers were re-digitised to assess the intra-investigator reliability of the kinematic measurement technique.

Measurement wheels and propulsion technique

The participant's right wheel was replaced with an instrumented wheel (SMARTWheel, 3-Rivers Holdings LLC, Mesa, AZ) (24/25"), which measured 3-dimensional forces and torques applied to the handrim, combined with the angle under which the wheel is rotated (**Appendix 1**). The left side was fitted with a weight-matched dummy. Data from the instrumented wheel were wirelessly transmitted to a laptop at 100Hz and analysed using custom-written Matlab routines (Vegter et al. 2013). To be certain of stable, steady state wheelchair propulsion, force (N), torque (Nm), angle (deg) and time (s) from the final minute for each speed and participant were used for further analyses. Individual push phases were defined as each period of continuous positive torque around the wheel axis with a minimum of at least 1Nm. One propulsion cycle was determined as the period between a positive torque around the wheel and the next positive torque around the wheel. Over the identified pushes the propulsion technique variables were calculated and subsequently averaged over all pushes in the third minute of each trial (**Table 2**).

Table 2 Description of propulsion parameters derived from the instrumented wheel

Variable	Description
Frequency (push/min)	Total pushes per minute
Cycle time (s)	Time from the start of positive torque to the next start of positive torque
Push percentage cycle time (%)	Relative proportion of cycle time spent during push phase
Contact angle (˚)	Angle on the wheel at the end of a push minus the angle at the start
Peak force (N)	Total 3-dimensional peak force during the push phase
Mean fraction of effective force (FEF) (%)	Fraction of total force acting tangentially to the wheel during the push phase

Kinematic data processing

The orientation and position of the scapula and humerus were defined in respect to the ISB recommendations (Wu et al. 2005). The scapula coordinated system was defined as follow:

$$Z_s = \frac{\mathrm{AA} - \mathrm{TS}}{|AA - TS|}, \quad X_s = \mathrm{Z}_S \times \frac{\mathrm{AI} - \mathrm{TS}}{|AI - TS|}, \quad Y_s = Z_s \times X_s$$

The humeral coordinated system was defined as follow:

$$Y_H = \frac{\mathrm{GH} - \mathrm{EJC}}{|\mathrm{GH} - \mathrm{EJC}|}, \quad X_H = \mathrm{Y}_H \times \frac{\mathrm{LE} - \mathrm{ME}}{|LE - ME|}, \quad Z_H = X_H \times Y_H$$

Euler angles were used to describe the relative movement of the scapula compared to the thorax (ST) across the propulsion cycle. The ISB guidelines were used to describe scapula orientation relative to the thorax (YXZ) as internal/external rotation (Y), upward/downward rotation (X) and posterior/anterior tilting (Z) (**Appendix 2)** (Wu et al. 2005). To provide ST rotations for both the left and right side, the left extremity markers were mirrored with respect to the thorax. Fifty consecutive propulsion cycles were selected from the final minute of each trial, each of these cycles was normalised from 0 to 100% with an increment of 1%. Average and standard deviation of the fifty cycles for each condition (T1 and T2) and each speed were calculated.

Statistical analysis

All statistical analysis was performed using statistical package IBM SPSS Statistics for Windows (Version 22, IB Corp., Armonk, N.Y, USA). Normal distribution of the outcome variables was confirmed for all data using a Shapiro-Wilk test. Mean propulsion kinetics and scapular kinematics were compared between T1 and T2 using students-paired T-Test. Propulsion technique and kinetics as well as scapular kinematic data (mean and peak data, absolute bilateral asymmetries) were analysed across submaximal speeds using a one-way repeated measures analysis of variance (ANOVA). Where significant F ratios were shown, Tukey post hoc tests were employed to determine where changes existed across speeds. For comparisons where the assumption of sphericity was violated, a Greenhouse-Geisser correction was applied. Significance was set *a priori* at $p \leq 0.05$. Effect sizes (ES) (partial eta^2) are presented, whereby 0.2 refers to a small effect, 0.5 refers to a moderate effect, and 0.8 refers to a large effect according to Cohen (1992). Reliability of the AMC method was assessed in T1 versus T2 for each speed using intra-class correlation co-efficient (ICC) and typical error of the measurement (TE).

Results

Participant characteristics are shown in **Table 1,** including time spent as MWU, WUSPI response and bilateral PSQ. Five participants reported shoulder pain in the last 3 months according to the PSQ (range 2 (low) to 15 (high)), of which three presented unilateral pain and two bilateral pain. The three participants with most severe PSQ shoulder pain (≥6) also reported highest WUSPI pain (≥22). All subjects were able to successfully complete all of the submaximal stages. Technological errors meant data from 3 participants was unavailable for T1. No significant differences were identified between all propulsion technique parameters and scapular kinematic measurements between T1 and T2 (n=7), therefore only means and standard deviation for T2 data are presented. ICC for scapular kinematic reliability (T1 vs. T2, right side only) ranged from 0.87 to 0.97 with a TE from 1.3º to 3.1º (**Table 3**).

The influence of propulsion speed on both technique related parameters and kinetics are shown in **Table 4**. Push frequency, peak force, contact angle, cycle time and power output were all significantly influenced by propulsion speed ($p<0.05$; ES = >0.38). Mechanical efficiency and mean FEF showed no change with propulsion speed. Mean and peak scapular kinematics for all submaximal speeds is shown in **Table 5**. Common to all speeds was an internally rotated, upwardly rotated and anteriorly tilted scapula. Mean ST rotations normalised over one push cycle (1-100%) at 6 km.h^{-1} are shown in **Figure 1**. At the end of the push phase and early in the recovery phase the scapula moved towards greater internal rotation and a neutral or slightly posteriorly tilted position. A small increase in upward rotation was also seen during the push phase. Mean (~3º) and peak (~4º) scapular internal rotations were significantly greater for the 6 km.h^{-1} trial than either of the other speeds. A moderate effect ($p=0.07$; ES =0.26) was seen for downward rotation at 6km.h^{-1} although this did not reach statistical significance (**Table 4**).

The absolute bilateral asymmetries (mean and range) in scapular kinematics across submaximal speeds are shown in **Table 6**. No differences in the magnitude of asymmetries were evident within the group data across speeds. Mean bilateral scapular kinematics for each individual participant at 6 km.h^{-1} are shown in **Figure 2**. A large inter-individual variability was observed for all ST rotations with no observable difference between those symptomatic and asymptomatic for shoulder pain.

Table 3 Intra-investigator reliability for scapular kinematics (T1 vs. T2) (n=7).

ST rotation		3 Km·h^{-1}	4^{-} Km·h^{-1}	6 Km·h^{-1}
Internal rot. (+)	**ICC**	0.87	0.90	0.93
External rot. (-)	**TE (º)**	3.1	2.6	2.4
Upward rot. (-)	**ICC**	0.90	0.92	0.97
Downward rot. (+)	**TE (º)**	2.6	2.2	1.6
Anterior tilt (-)	**ICC**	0.90	0.91	0.92
Posterior tilt (+)	**TE (º)**	2.5	2.5	1.9

n.b. TE = typical error; ICC = intraclass correlation coefficient

Table 4 Propulsion technique and kinetic parameters across three submaximal propulsion speeds

Outcome parameter	3 Km·h^{-1}	4^{-} Km·h^{-1}	6 Km·h^{-1}	Effect size (Partial ETA^2)
VO2 (L·min^{-1})	0.47 (0.11)*	0.59 (0.11)*	0.83 (0.14)*	0.68
Velocity (Km·h^{-1})	3.25 (0.06)*	4.19 (0.05)*	6.22 (0.09)*	0.98
Power (W)	9.1(1.3)*	12.1(1.4)*	18.3(2.6)*	0.96
Frequency (push·min)	52.2 (9.5)*	56.3 (8.7)*	65.7 (10.2)*	0.75
Cycle time (s)	1.04 (0.29)^	0.89 (0.17)^	0.77 (0.10)	0.52
Push percentage cycle time (%)	39.1 (5.6)*	35.6 (5.5)*	31.4 (5.5)*	0.80
Contact Angle (º)	84.1 (14.5)*	89.7 (14.0)*	93.39 (15.1)*	0.38
Peak force (N)	43.6 (9.6)*	51.3 (10.0)*	67.5 (16.07)*	0.68
Mean fraction of effective force (FEF) (%)	45.0 (10.0)	44.4 (7.8)	46.7 (8.6)	0.07
Mechanical efficiency (%)	5.9 (1.1)	5.8 (0.9)	6.4 (1.2)	0.20

n.b. * significantly different to both other speeds (<0.05); ^significantly different to 6 Km·h^{-1} ($p < 0.05$)

Table 5 Mean and peak scapular kinematics across three submaximal propulsion speeds

ST rotation		**3 Km·h^{-1}**	**4^{-} Km·h^{-1}**	**6 Km·h^{-1}**	**Effect size (Partial ETA^2)**
Internal rot. (+)	**Mean (º)**	29.7 (6.9)^	30.7 (6.6)^	32.8 (7.0)	0.66
External rot. (-)	**Peak (º)**	41.2 (7.9)^	42.9 (7.4)^	46.0 (6.1)	0.53
Upward rot. (-)	**Mean (º)**	-9.8 (8.8)	-9.8 (8.6)	-9.8 (9.1)	0.02
Downward rot. (+)	**Peak (º)**	-13.4 (10.2)	-13.1 (11.0)	-14.7 (8.1)	0.26
Anterior tilt (-)	**Mean (º)**	-7.2 (7.1)	-7.5 (7.5)	-7.5 (7.9)	0.04
Posterior tilt (+)	**Peak (º)**	-11.2 (11.1)	-10.7 (11.6)	-9.7 (12.3)	0.17

n.b. ^ significantly different to 6 Km·h^{-1} ($p < 0.05$)

Table 6 Absolute differences between bilateral scapular kinematics across three propulsion speeds

ST rotation		**3 Km·h^{-1}**	**4^{-} Km·h^{-1}**	**6 Km·h^{-1}**	**Effect size (Partial ETA^2)**
Internal rot. (+)	**Mean (º)**	5.7 (4.8)	6.6 (5.1)	5.8 (5.0)	0.13
External rot. (-)	**Range (º)**	1.1 to 15.1	1.2 to 16.7	0.5 to 14.3	-
Upward rot. (-)	**Mean (º)**	2.9 (2.8)	3.2 (3.2)	3.5 (2.1)	0.22
Downward rot. (+)	**Range (º)**	0.4 to 9.0	1.0 to 11.6	0.42 to 7.0	-
Anterior tilt (-)	**Mean (º)**	4.6 (2.4)	3.7 (2.7)	4.6 (2.8)	0.26
Posterior tilt (+)	**Range (º)**	0.9 to 9.7	0.1 to 9.9	1.1 to 10.7	-

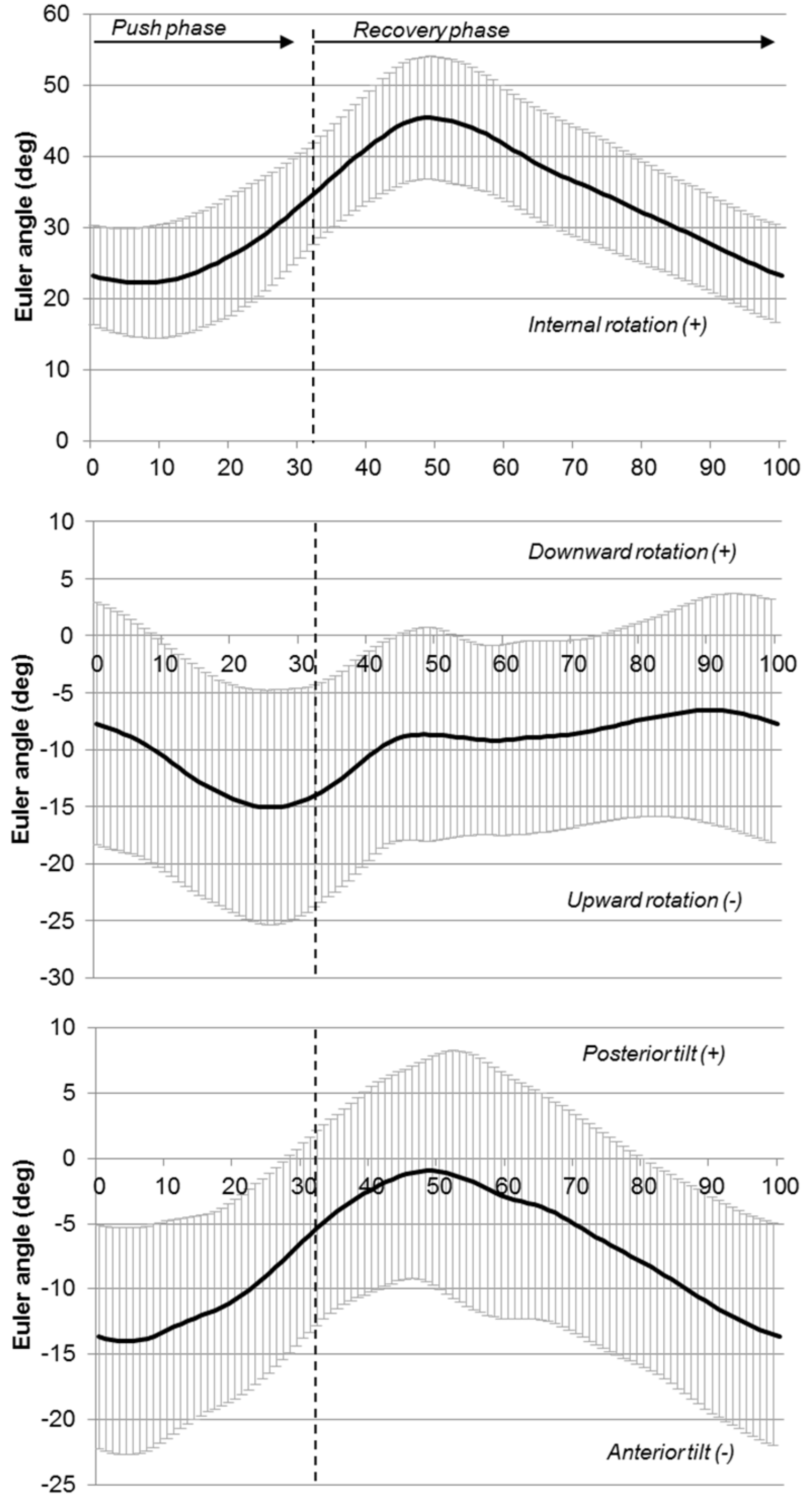

Figure 1 Mean (SD) scapular kinematics normalised (0-100%) to a whole propulsion cycle at 6 Km·h^{-1}. n.b. dashed line denotes end of push phase and transition to recovery phase, estimated from group cycle time data.

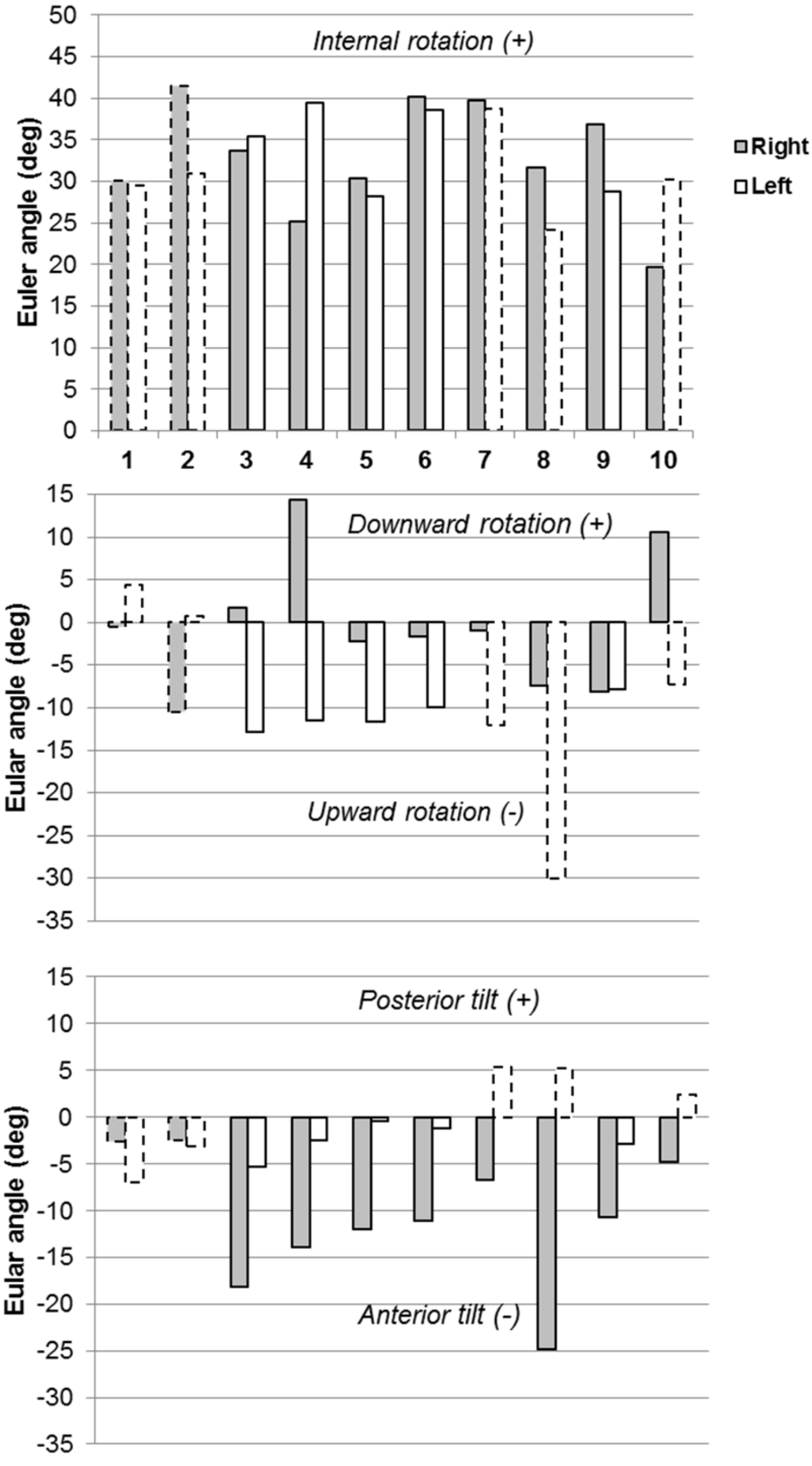

Figure 2 Individual participant (no. 1-10) mean scapular kinematics at 6 $Km \cdot h^{-1}$. n.b. dashed line denotes self-reported musculoskeletal shoulder pain according to PSQ (van Drongelen et al. (2006)).

Discussion

The overall objective of this PMG funded project was to establish the feasibility of a multi-system measurement of manual wheelchair prolusion kinetics and kinematics. Of particular interest was the reliability of the AMC method for the bilateral assessment of three-dimensional scapular motion during MWU. The initial findings of this work will inform future well-designed, scientific data collection prioritising pain reduction and associated secondary conditions by optimising the configuration of manual wheelchairs.

Using previously established methodology (van der Woude et al. 2009; Veeger et al. 2002), wheelchair propulsion technique and kinetics were examined across three submaximal propulsion speeds associated with ADL. We recruited ten physically active males experienced in manual propulsion, 8 of which had a cervical spinal cord injury. An increased propulsion frequency and contact angle on the handrim was observed with increasing propulsion speed, despite a reduction in hand contact time. Increasing contact angle acts to increase the distribution of force over the propulsion cycle and may in turn reduce GH reaction forces (Russell et al. 2015; Vegter et al. 2013). However, peak forces applied to the hand-rim also increased significantly with speed, increasing the challenge for the muscles of the shoulder girdle to maintain joint stability (Koontz et al. 2002). Previously Kulig et al. (2001) reported significantly higher peak superior joint forces in MWU with tetraplegia than paraplegia at a given self-selected propulsion velocity. A lack of grip function on the wheel early in the push phase in individuals with C7 tetraplegia may subsequently lead to a compensatory increased force production later in the push phase (Kulig et al. 2001). This superior push force coupled with the weakness in of thoracohumeral depressors increase the susceptibility of the subacromial structures to compression in this population (Kulig et al. 2001; Raina et al. 2012). Wheelchair configuration, including seat height and axle position relative to the UE, is also known to influence propulsive shoulder girdle forces via influences on rolling resistance and handrim contact angle (Boninger et al. 2000, van der Woude et al. 2009). Therefore, understanding the forces acting on the UE during manual propulsion is a vital component of addressing pain and UE injury risk with different chair configurations.

The morphology and position of the scapula as well as its complex motion mean it is very challenging to track using motion capture technology. The development of the AMC minimises the influence of skin motion artefact during dynamic propulsion but relies on the flat superior aspect of the acromion to reflect total scapular movement (van Andel et al.2009;

Warner et al. 2012). The validity and reliability of the AMC method has previously been confirmed against 'gold-standard' bone-pin measurements during humeral-elevation activity under 120˚ (van Andel et al. 2009). However, this does not account for the substantial vibrations and muscle activity during dynamic propulsion which may influence contact been the AMC and skin (Warner et al. 2012). Despite the limited reliability AMC measures have been frequently used for the measurement of scapular kinematics during manual propulsion (Raina et al. 2002; Zhao et al. 2015). Understanding the error within a measurement is vital to interpreting the clinical relevance of findings and the success of any intervention. The intra-observer reliability data reported here suggest good reproducibility of the AMC method under submaximal propulsion conditions, with ICC with 0.87-0.97 and a typical error never exceeding ~3˚ (**Table 3**).

In agreement with previous findings, mean and peak kinematics across all speeds showed an internally and upwardly rotated scapula with anterior tilt (Raina et al. 2012; Zhao et al. 2014). As shown in **Figure 1**, relatively small magnitudes of change were observed over the propulsion cycle with the scapula moving to a position of peak internal rotation and reduced anterior tilt early in the recovery phase. A scapula position of less upward rotation and increased internal rotation, commonly seen in scapula dyskinesis, increases the area of contact of between the humerus with the posterior superior glenoid (Kilber et al. 2013). The combination of scapular orientation and forces acting on the shoulder girdle helps define the risk of impingement pathology during manual wheelchair propulsion and other ADL, including transfers and weight relief (Morrow et al. 2011). Novel to this study was the collection of scapular kinematic data of participants with tetraplegia in their own manual wheelchair (Raina et al. 2012). This is important given the influence of impaired trunk function and therefore postural position on scapular and UE motion in this population group, adding ecological validity to our findings.

Of interest is the difference in scapular motion between different levels of spinal cord injury. Previously, Raina et al. (2012) reported a greater rate of change in scapular kinematics (particularly internal rotation) for individuals with tetraplegia than paraplegia. This may reflect a lack of scapular stability through alterations in rotator cuff or other scapular stabiliser function, including serratus anterior or the upper and lower trapezius (Mulroy et al. 2004). Interestingly, there was a large intra-individual variation in scapular motion observed by Raina et al. (2012) in participants with tetraplegia. This is supported in our individual findings shown in **Figure 2**, especially for upward/downward rotation. Serratus anterior activation and strength is decreased in patients with impingement and shoulder pain, contributing to the loss of posterior tilt and upward rotation causing scapular dyskinesis (Ludewig and Cook 2000). Inflexibility and stiffness of the pectoralis minor and biceps short head can create anterior tilt and protraction due to their pull on the coracoid process (Kilber et al. 2013). Understanding the exact reasons for observed scapular kinematics requires individual analysis depending on injury level, push technique and rotator cuff muscle strength, rather than the grouping of data. Future research must also be done to with accurate methods of quantifying subacromial space to identify if the scapular movement during MWU is clinically relevant.

The presence of bilateral asymmetries in kinetics and kinematics has received relatively little attention in the large volume of wheelchair propulsion literature (Boninger et al. 2002; Hurd et al. 2008; Soltau et al. 2015; Vegter et al. 2013). A substantial proportion of self-reported shoulder pain is unilateral in nature (Curtis et al. 1999), which is supported by the findings from our small cohort of participants. **Table 6** shows the absolute magnitude of scapular kinematic asymmetries (no accounting for direction), while **Figure 2** displays the magnitude of bilateral asymmetry for each individual at the fastest speed performed. Previously, Hurd et al. (2008) reported the magnitude of asymmetry in propulsion kinetics increased with the mechanical load (ramp pushing, uneven terrain) of a propulsion task. In contrast, our findings show no increase in the absolute magnitude of asymmetries with propulsion speed. However, the individual magnitude of bilateral variation observed in the scapular kinematic reported here are much greater than the ~5° difference in UE joint range observed by Soltau et al. (2015). No observable relationship was present between scapular asymmetries and the presence of self-reported pain in this cohort. It remains unknown whether asymmetries may be a cause of UE pain or simply a compensatory measure to reduce symptoms. Further work should focus on the range of observable asymmetries in MWU and their association with pain in order to determine whether they are clinically meaningful on an individual basis. This is especially important in individuals with tetraplegia who may present bilateral deficits in shoulder girdle strength and where observing grouped cohort data may hide individual prevalence.

Future focus

Given the limited time-scale available to the project group (December 2015-July 2016), further exploration of muscle activity (surface electromyography (sEMG)) and joint loads (GH joint moments) will be performed following the submission of this final report.

Computer-based, inverse dynamic modelling techniques will be employed to quantify the moments and forces acting upon the shoulder complex using hand-rim kinetics and UE kinematics. The complex analysis was beyond the scope of this current work but can be used to describe the individual scapular kinematics reported above. In addition, analysis of sEMG data from 8 muscle groups (biceps, triceps, anterior deltoid, middle deltoid, serratus anterior, lower trapezius, upper trapezius and pectoralis major) will support the understanding of individual motor control and muscle loading during bimanual wheelchair propulsion.

Conclusions

This project performed a comprehensive analysis of wheelchair propulsion kinetics and scapular kinematics in a small cohort of MWU, experienced in manual wheelchair use for sport and ADL. The findings confirmed the reliability of the AMC for quantifying scapular kinematics during submaximal wheelchair propulsion and highlight the importance of bilateral observations of UE kinematics, especially in individuals with tetraplegia. This work has established methods and generated an initial database to enable future work understanding how wheelchair configurations can be manipulated to prevent shoulder girdle pain and improve propulsive efficiency. Further we have a robust measurement protocol which can be refined in future so real time information can be generated to assess the effectiveness of manipulations in manual wheelchair configuration.

Acknowledgements

We would like to thank Dr Jan van der Scheer and Miss Marika Leving for their contribution to experimental data collection and analysis. We are also very grateful to the support from Great Britain Wheelchair Rugby and the participants who volunteered their time to take part in the study.

References

Arnet, U., van Drongelen, S., Scheel-Sailer, A., van der Woude, L.H.V & Veeger, H.E.J. (2012) Shoulder load during synchronous handcycling and handrim wheelchair propulsion in persons with paraplegia. *Journal of Rehabilitation Medicine*. 44:222-228.

Boninger, M.L., Baldwin, M., Cooper, RA., Koontz, A. & Chan, L. (2000) Manual wheelchair pushrim biomechanics and axle position. *Archives of Physical Medicine and Rehabilitation*. 81, 608-613.

Boninger, M.L., Souza, A.L., Cooper, R.A., Fitzgerald, S.G., Koontz, A.M. & Fay, B.T. (2002) Propulsion patterns and pushrim biomechanics in manual wheelchair propulsion. *Archives of Physical Medicine and Rehabilitation.* 83, 718-723.

Brose, S.W., Boninger, M.L., Fullerton, B., McCann, T., Collinger, J.L., Impinil, B.G. & Dyson-Hudson, T.A. (2008) Shoulder ultrasound abnormalities, physical examination findings and pain in manual wheelchair users with spinal cord injury. *Archives of Physical Medicine and Rehabilitation*. 89, 2086-2093.

Capozzo, A. Catanl, F., Della Croce, U. & Leardini, A. (1995) Position and orientation in space of bones during movement: anatominal frame definition and determination. *Clinical Biomechanics*. 10(4), 171-178.

Cohen, J. (1992) A power primer. *Quantitative Methods in Psychology*. 112(1), 155-159.

Curtis, K.A., Roach, K.E., Applegate, E.B., Amar, T., Benhow, C., Genecco, T.D. & Gualano, J. (1995) Reliability and validity of the wheelchair users shoulder pain index (WUSPI). Paraplegia. 33: 595-601.

Curtis, K.A., Dysdale, G.A., Lanza, R.D., Kolber, M., Vitolo, R.S. & West, R. (1999) Shoulder pain in wheelchair users with tetraplegia and paraplegia. *Archives of Physical Medicine and Rehabilitation*. 78:435:446.

Eriks-Hoogland, I., de Groot, S., Snoek, G., Stucki, G., Post, M. & van der Woude, L. (216) Association of shoulder pain in persons with spinal cord injury at discharge from inpatient rehabilitation with activities and participation 5 years later. *Archives of Physical Medicine and Rehabilitation.* 97, 84-91.

Hurd, W.J., Morrow, M.M., Kaufman, K.R. & An, K-N. (2008) Biomechanic evaluation of upper-extremity symmetry during manual wheelchair propulsion over varied terrain. *Archives of Physical Medicine and Rehabilitation.* 89, 1996-2002.

Karduna, A.R., McClure, P.W., Michener, L.A. & Sennet, B. (2001) Dynamic measurements of three-dimensional scapular kinematics: A validation study. *Journal of Biomechanics*. 123(2), 184-190.

Koontz et al. (2002) Shoulder kinematics and kinetics during two speeds of wheelchair propulsion. Journal of Rehabilitation Research and Development. 39(6):635-650.

Kibler, W.B., Ludewig, P.M., McClure, P.W., Michener, L.A., Bak, K. & Sciascia, A.D. (2013) Clinical implications of scapular dyskinesis in shoulder injury: the 2013 statement from the ‘scapular summit’. *British Journal of Sports Medicine.* doi:10.1136/bjsports-2013-092425.

Kulig, K., Newsam, C.J., Mulroy, S.M., Rao, S., Gronly, J.K., Bontrager, E.L. & Perry. J. (2001) The effect of level of spinal cord injury on shoulder joint kinetics during manual wheelchair propulsion. *Clinical Biomechanics*. 16, 744-751.

Ludewig, P.M. & Cook, T.M. (2000) Alterations in shoulder kinematics and associated muscle activity in people with symptoms of shoulder impingement. *Physical Therapy*. 80, 276-291.

Medina, G.I.S, Jesus, C.L.M., Ferreira, D.M., Pacheco, E.M.B., Beraldo, G.L., de Franca Urquiza, G.L. & Cliquet, A. (2015) Is sport practice a risk factor for shoulder injuries in tetraplegic individuals? *Spinal Cord*. 53, 461-466.

Meskers, C.G.M, van der Helm, F.C.T., Rozendaal, L.A. & Rozing, P.M. (1998) In vivo estimation of the glenohumoral joint rotation center from scapular bony landmarks by linear regression. *Journal of Biomechanics*. 31,93-96.

Morrow, M.M.B., Kaufman, K.R. & An, K-N. (2011) Scapula kinematics and associated impingement risk in manual wheelchair users during propulsion and weight relief lift. Clinical Biomechanics. 26:352:357.

Mulroy, S,J., Farrokhi, S., Newsam, C.J. and Perry, J. (2004) Effects of spinal cord injury level on the activity of the shoulder muscles during wheelchair propulsion: An electromyographic study. *Archives of Physical Medicine and Rehabilitation*. 85, 925-934.

Nichols, P.J., Norman, P.A., & Ennis, J.R. (1979) The wheelchair user’s shoulder? Shoulder pain in patients with spinal cord injury. *Scandinavian Journal of Rehabilitation Medicine*. 11:29-32.

‘Right chair, Right now’ NHS improving quality 2014.

Raina, S., McNitt-Gray, J.L., Mulroy, S. & Requejo, P.S. (2012) Effect of increased load on scapular kinematics during manual wheelchair propulsion in individuals with paraplegia and tetraplegia. *Human Movement Science*. 31, 397-407.

Russell, I.M., Raina, S., Reuejo, P.S., Wilcox, R.R., Mulroy, S. & McNitt-Gray, J.L. (2015) Modifications in wheelchair propulsion technique with speed. *Frontiers in Bioengineering and Biotechnology*. 3,171.

Soltau, S.S., Slowik, J.S., Reuejo, P.S., Mulroy, S.J. & Neptune, R.R. (2015) An investigation of bilateral symmetry during manual wheelchair propulsion. *Frontiers in Bioengineering and Biotechnology*. 3,96.

van Andel, C., van Hutten, K., Eversdijk, M., Veeger, H.E.J. & Harlaar, J. (2009) Recording scapular motion using an acromion marker cluster. *Gait and Posture*. 29, 123-128.

van Drongelen, S., de Groot, S., Veeger, H.E.J., Angenot, E.L.D., Dallmeijer, A.J., Post, M.W.M. & van der Woude, L.H.V. (2006) Upper extremity pain during and after rehabilitation in wheelchair-using persons with a spinal cord injury. *Spinal Cord.* 44, 152-159.

van der Woude, L.H.V., Veeger, H.E.J., Rozendal, R.H. & Sargeant, T.J. (2009) Seat height: effects on submaximal hand rim wheelchair performance during spinal cord injury rehabilitaiton. *Journal of Rehabilitation Medicine.* 41, 143-149.

Veeger, H.E.J., Rozendaal, L.A., & Helm van der, F.C.T. (2002) Load on the shoulder in low intensity propulsion. *Clinical biomechanics.* 17, 211-218.

Veeger, H.E.J. & Helm van der, F.C.Y (2007) Shoulder function: The perfect compromise between stability and mobility. *Journal of Biomechanics*. 40, 2119-2129.

Vegter, R.J.K, Lamoth, C.J.C, de Groot, S., Veeger, H.E.J. & van der Woude, L.H.V. (2013) Variability in bimanual wheelchair propulsion: consistency of two instrumented wheels during handrim wheelchair propulsion on a motor drive treadmill. *Journal of NeuorEngineering and Rehabilitation.* 10(9).

Vegter, R.J.K., Hartog, J., de Groot, S., Lamoth, C.J., Bekker, M., van der Scheer, J.W., van der Woude, L.H.V. & Veeger, D.H.E.J (2015) Early motor learning changes in upper-limb dynamics and shoulder complex loading during handrim propulsion. *Journal of Neuroengineering and Rehabilitation*. 12-26.

Warner, M., Chappell, P.H. & Stokes, M.J. (2012) Measuring scapular kinematics during arm lowering using the acromion marker cluster. *Human Movement Science.* 31, 386-396.

Whipp, B.J., & Wasserman, K. (1969) Efficiency of muscular work. *Journal of Applied Physiology*. 26(5), 644-648.

Wu, G., van der Helm, F.C.T., Veeger, H.E.J., Makhsous, M., van Roy, P., Aglin, C et al. (2005) ISB recommendation on definitions of joint co-ordinate systems of various joints for the reporting of human joint motion – Part II: shoulder, elbow, wrist and hand. *Journal of Biomechanics.* 38, 981-992.

Zhao, K.D., van Straaten, M.G., Cloud, B.A., Morrow, M.M., An, K-N. & Ludewig, P.M. (2015) Scapulothoracic and glenohumoral kinematics during daily tasks in users of manual wheelchairs. *Frontiers in Bioengineering and Biotechnology*. 3, 183.

Appendix 1

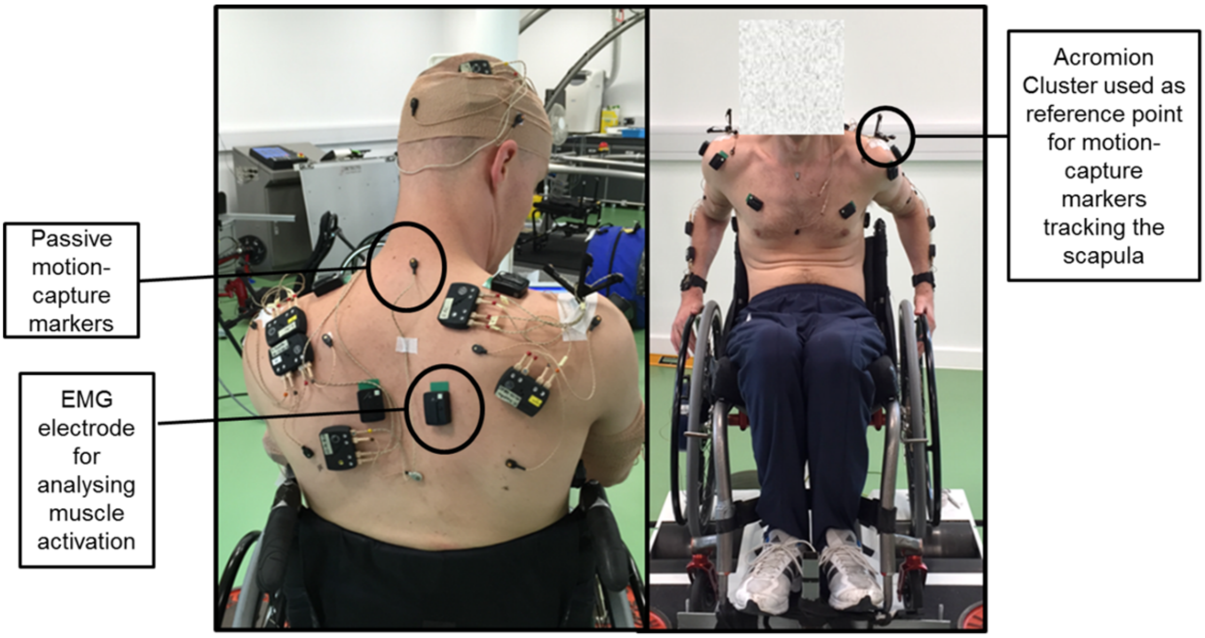

Figure 1. Participant preparation and placement of EMG and passive motion-capture markers

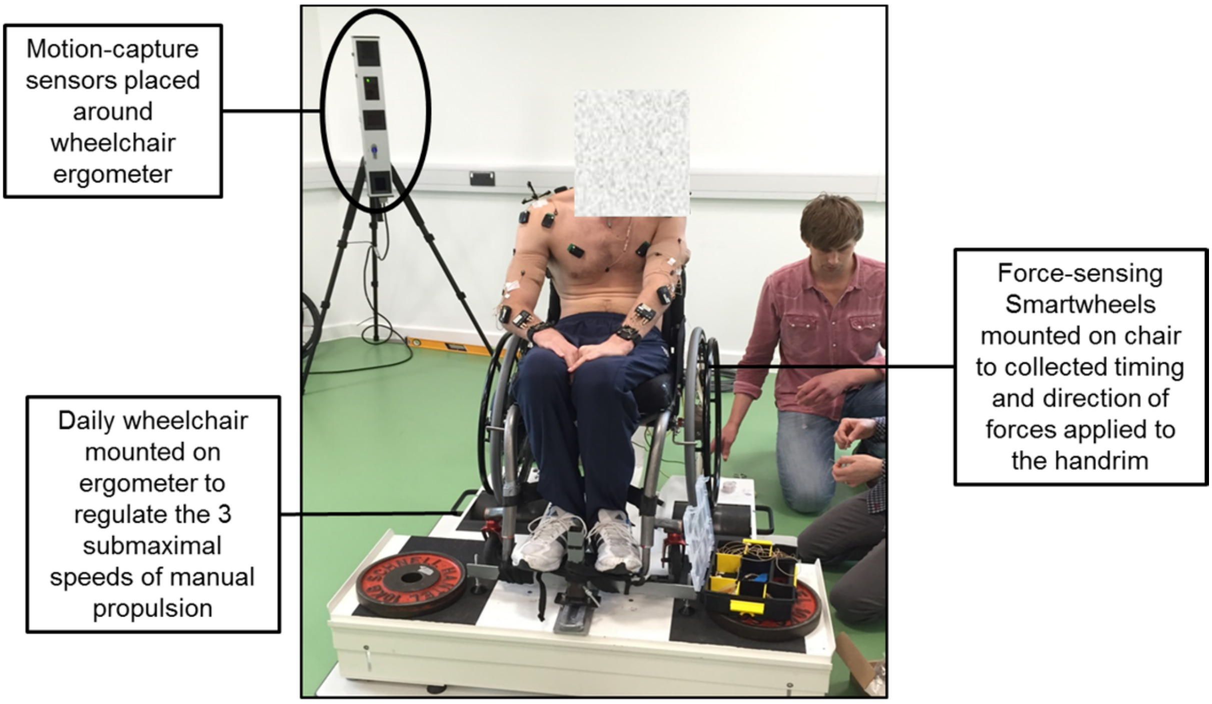

Figure 2. Experimental setup with wheelchair ergometer and motion-capture sensors

Appendix 2

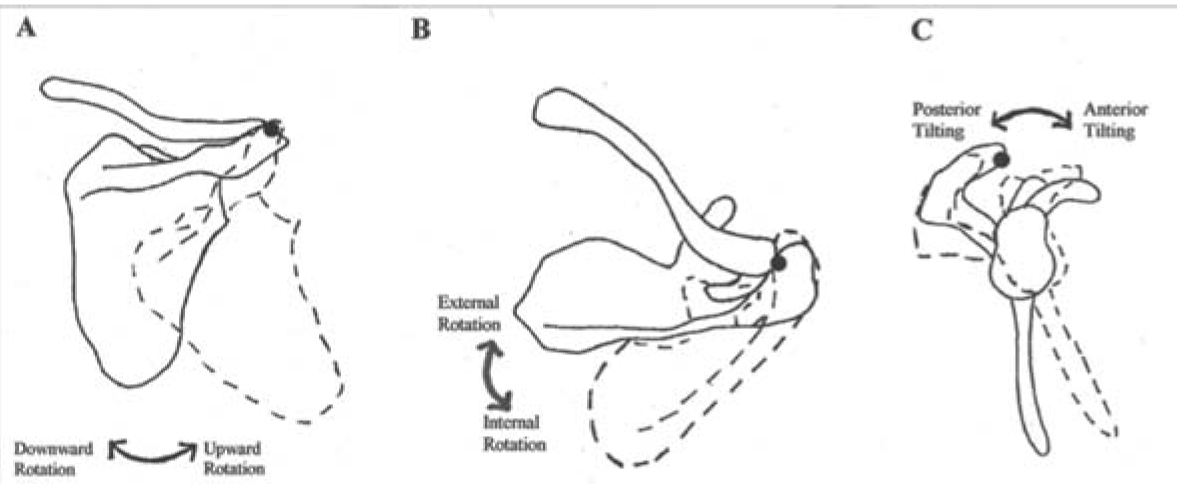

Reprinted from Borich MR, Bright JM, Lorello DJ, Cieminski CJ, Buisman T, Ludewig PM. Scapular angular positioning at end range internal rotation in cases of glenohumeral internal rotation deficit. J Orthop Sports Phys Ther. 2006;36(12):926-34, with permission of the Orthopaedic and Sports Physical Therapy Sections of the American Physical Therapy Association.